Oxidative Stress Induced by Zero-Valent Iron Nanoparticles and Fe(II) in Human Bronchial Epithelial Cells: Supporting Information

*Christina R. Keenan[1], Regine Goth-Goldstein[2], Donald Lucas[3], and David L. Sedlak[1,]**

[1] Department of Civil and Environmental Engineering

University of California at Berkeley

Berkeley, California 94720

[2] Environmental Energy Technologies Division

Lawrence Berkeley National Laboratory

Berkeley, California 94720

[3] Environmental Health and Safety Division

Lawrence Berkeley National Laboratory

Berkeley, California 94720

Submitted to *Environmental Science & Technology* on March 2, 2009.

Contents (19 pages):

Figures S1-S7 and Tables S1-S2

* Corresponding author e-mail: sedlak@ce.berkeley.edu; telephone: (510) 643-0256; fax: (510) 642-7483.

Materials and Methods

Materials

All chemicals were reagent grade and were used as received except 2,4-dinitrophenyl hydrazine (DNPH), which was recrystallized three times from acetonitrile. All solutions were prepared using 18 MΩ Milli-Q water from a Millipore system. Glassware for cell-free experiments and iron analysis was acid-washed and rinsed before use. Glassware for solution preparation for the lung cell experiments was autoclaved after acid-washing.

Phosphate-buffered saline (PBS: 1.06 mM KH_2PO_4, 2.97 mM Na_2HPO_4, 155 mM NaCl) with the pH adjusted to 7.0 with HCl, was used in all experiments, unless indicated. PBS was chosen because it is the simplest solution that adequately buffers the system when nanoparticulate zero-valent iron (nZVI) is added and provides conditions conducive to bronchial epithelial cell viability. As described in the manuscript, oxidant yield during nZVI oxidation was enhanced in PBS relative to PIPES-buffered solutions used in previous studies [1-2]. Iron chelators, such as 2,2'-bipyridine (BPY) or desferrioxamine (DFO), or oxidant scavengers, such as dimethyl sulfoxide (DMSO), benzoate (BA), or *tert*-butanol (TBA), were added to PBS in some experiments (Table S1). PBS solutions for the lung cell experiments were autoclaved or filter-sterilized, as appropriate.

Nanoparticulate zero-valent iron was prepared daily as described previously to produce primary particles with a diameter between 10 and 100 nm and a surface area of 33.5 m^2/g [3-4]. The primary particles aggregate into chains in solution [3]. Ferrous iron (Fe[II]) stock solutions were prepared by dissolving ferrous sulfate in 1 mM HNO_3. Weathered nZVI suspensions were prepared by allowing the diluted nZVI solution to oxidize in air-saturated PBS solutions for 4 h

prior to use. Measurements of Fe(II) indicated that all of the iron was oxidized within this period.

Cell-free experiments

Experiments in the absence of cells were carried out in air-saturated solutions at room temperature (20 ± 2ºC) in the dark, except as noted. The 60-mL glass serum vials were sealed with rubber septa with no headspace to prevent oxygen transfer to and from the solution. Although the concentration of oxygen decreased as iron was oxidized, the final [O_2] was never less than 50 μM. To initiate a reaction, an aliquot of nZVI and/or Fe(II) was added from a stock solution to solutions containing 5-100 mM of the probe compound in a buffer solution (e.g., PBS, PIPES). The particles were kept in suspension by placing the reactors on an orbital shaker table at 150 rotations per minute. Samples were collected at different time intervals using a 5-mL glass syringe and filtered immediately through a 0.22-μm nylon syringe filter (Fisher). The reactors were sacrificial, at least three reactors were sampled for each time point, and the data were averaged.

Equilibrium speciation calculations were performed using MINEQL+, with equilibrium constants added from the NIST Standard Reference Database [5] as necessary.

A colorimetric method [6], was used to quantify filterable Fe(II), total filterable iron, and total iron in experiments conducted in the absence of 2,2'-bipyridine or desferrioxamine. The method was further modified by adding an aliquot of ammonium fluoride (final concentration = 7 mM) before adding ferrozine to dissolved Fe(II) samples to prevent interference by Fe(III). Filterable iron was defined as iron that passed through a 0.22-μm nylon syringe filter. Total iron was quantified after adding hydroxylamine hydrochloride (final concentration = 60 mM) to acidified samples. Control experiments with freshly prepared nanoparticles indicated that nZVI did not

pass through the filter (data not shown). Samples were analyzed on a UV-Vis spectrophotometer (Perkin Elmer Lambda 14; $\varepsilon_{562\ nm}$ = 27,900 M^{-1} cm^{-1}) with a 1-cm pathlength cuvette. All standard curves were linear with regression coefficients >0.9990 and a detection limit of 0.2 μM.

Complexes of 2,2'-bipyridine (BPY) with Fe(II) or desferrioxamine (DFO) with Fe(III) form a pink or orange color, respectively, that can be quantified spectrophotometrically. In experiments with BPY, samples were filtered and acidified to measure filterable Fe(II) or reduced with hydroxylamine hydrochloride to measure total filterable iron. Total iron was quantified after adding hydroxylamine hydrochloride (final concentration = 60 mM) to acidified samples. The pH was raised to 4.7 using an ammonium acetate buffer (3.86 g ammonium acetate and 2.83 mL of 30% NaOH/10 mL). In experiments with DFO, total filterable and total iron were measured by acidifying filtered or unfiltered samples and then raising the pH with an ammonium acetate buffer. Samples were analyzed on a UV-Vis spectrophotometer. The detection limits were 0.4 and 0.8 μM for Fe(II) in BPY ($\varepsilon_{523\ nm}$ = 9,100 M^{-1} cm^{-1}; [7]) and Fe(III) in DFO ($\varepsilon_{425\ nm}$ = 2,460 M^{-1} cm^{-1}; [8]), respectively.

Superoxide production was quantified by measuring the colored product of the reaction of 3'-[1-[(phenylamino)-carbonyl]-3,4-tetrazolium]-bis(4-methoxy-6-nitro)benzene-sulfonic acid hydrate (XTT) reduction with $O_2^{-\bullet}$ ($\varepsilon_{470\ nm}$ = 21,600 M^{-1} cm^{-1}; [9-10]). The concentration of superoxide was determined by comparing XTT reduction by nZVI with and without 30 U/mL superoxide dismutase (MP Biomedicals) to account for XTT reduction by sources unrelated to $O_2^{-\bullet}$. Samples were prepared by mixing 100 μM nZVI with 300 μM XTT in PBS in 25 mL glass flasks. Samples were mixed on a stir plate in the dark, with six replicates for each condition. Aliquots were filtered at the appropriate time point and analyzed on a UV-Vis

spectrophotometer. The detection limit for reduced XTT was 0.7 μM, and should be identical to the $O_2^{-\bullet}$ detection limit assuming all of the $O_2^{-\bullet}$ produced resulted in reduction of XTT.

Hydrogen peroxide was measured using a modified N,N-dimethyl phenylendiamine (DPD) method [6, 11-12] with BPY added to complex Fe(II) and EDTA added to complex Fe(III). Samples were prepared by adding 100 μM nZVI to PBS; one set of samples contained 1mM 1,10-phenathroline to complex Fe(II) and prevent H_2O_2 loss. Samples were mixed on a stir plate in the dark, with three replicates for each condition. Aliquots were filtered at the appropriate time point and analyzed on a UV-Vis spectrophotometer. The procedure consisted of the following steps: first, 2 mL filtered sample was mixed with 200 μL BPY (20 mM in 1 mM HCl) to complex Fe(II), followed by the immediate addition of 100 μL EDTA (100 mM) to complex Fe(III). Next, 400 μL of phosphate buffer (pH 6.0, 0.5 M) was added. 10 μL of DPD (1% in 0.1 M H_2SO_4) was added and the absorbance at 551 nm was recorded for 1 min to determine the baseline absorbance. Finally, 10 μL of POD reagent (Peroxidase, Type 1 from Horseradish, Sigma, 113 units/mg; 90 U/mL) was added and the absorbance was monitored at 551 nm for an additional 2 min. The concentration of H_2O_2 was determined by subtracting the baseline absorbance from the stabilized absorbance after POD addition (ε = 21,000 M^{-1} cm^{-1}) [12]. The method detection limit was 0.4 μM.

Methanol and benzoate were used as probe compounds to quantify oxidant production and determine the nature of the reactive oxidant. Methanol is oxidized by either $OH^{\bullet}$ or Fe(IV), while benzoate reacts with $OH^{\bullet}$ but not Fe(IV) [1]. The main products from the oxidation of probe compounds were measured by HPLC as described previously [1]. High concentrations of methanol (100 mM) were used to ensure that the oxidants produced by Fe(II) oxidation reacted with the methanol to produce formaldehyde (HCHO). A lower concentration of benzoate (5

mM) was used due to its limited solubility, and under our experimental conditions, between 80 and 95% of the oxidants reacted with benzoate to form three isomers of hydroxybenzoate (ortho, meta, and para) in a ratio of 36:34:30 based on results of a previous study in which H_2O_2 photolysis was used as a $OH^{\bullet}$ source [13]. Total hydroxybenzoate (HBA) production was estimated from this ratio using measurements of *para*-hydroxybenzoate (pHBA). Competition experiments were performed with methanol and DMSO or TBA. During these experiments, only HCHO, the product of methanol oxidation, was monitored.

Cytotoxicity experiments

The human bronchial epithelial cell line 16HBE14o (immortalized by SV40 transformation) was used for the exposure experiments. These cells have been used in previous studies to investigate the cytotoxicity of other particles, including diesel exhaust particles [14-16] and a particulate fungicide [17], and to investigate oxidative stress caused by cigarette smoke [18] and H_2O_2 [19]. Cells were grown in collagen-coated flasks in minimum essential medium (MEM) substituted with 10% fetal bovine serum (Gibco), glutamine, and antibiotics (100 U mL^{-1} penicillin, 100 ug mL^{-1} streptomycin) and were maintained in the logarithmic phase of growth, with two separate batches used during the study. The cells were incubated at 37^{o}C in a 5% CO_2 atmosphere until a confluent layer of cells was achieved.

Cells were seeded into 12- and 24-well plates (with 4 and 1.9 cm^2 growth area, respectively) at a density of 0.5-1 x 10^5 cells per well two days before exposure to nZVI and Fe(II). Immediately before exposure, cells were rinsed with PBS. For all cytotoxicity experiments, PBS or PBS containing the appropriate scavenger or iron-chelator were used as controls. Fenton's reagent (100 μM Fe[II] and 1 mM H_2O_2 in PBS) was used as a positive control. During the one hour exposure to iron, cells were incubated at 37^{o}C in an incubator with ambient CO_2 concentrations

to prevent $FeCO_{3(s)}$ precipitation. The nominal iron concentration was verified by acidifying an aliquot of nZVI, Fe(II), or weathered nZVI stock solutions and measuring the total iron concentration. There were at least three wells per condition and Student's t-test was used to test statistical significance.

Cytotoxicity was measured by quantifying lactate dehydrogenase (LDH) released into solution during the one-hour exposure to nZVI, Fe(II) or weathered nZVI in PBS using a commercially available kit (Sigma Aldrich). The samples were centrifuged at 1,040 rpm for 10 min prior to LDH analysis and LDH was measured in the supernatant. At least three wells were used per dose and additional wells were treated with a lysis solution to measure total LDH and total cell number. Results are expressed as a percentage relative to the negative control and total LDH.

The 2'7'-dichlorodihyrdofluorescein diacetate (HDCF-DA) assay [20-23] was used in some experiments to measure ROS production inside the lung cells. Cells were incubated with 50 μM HDCF-DA in PBS for 60 min in the dark to allow the cells to take up the dye and cleave off the acetate groups, resulting in uptake of the free, reduced dye (2'7'-dichlorodihydrofluorescein, HDCF) to the cells. The cells were washed with PBS to remove excess dye and then exposed to the appropriate control or iron dose for 60 min. During the exposure, oxidants produced inside the cells could oxidize the reduced dye, HDCF, to a fluorescent product (2'7'-dichlorofluroescein, DCF). After the exposure, the solution was replaced with fresh PBS and fluorescence was measured at 528 nm with excitation at 485 nm using a Perkin Elmer Victor3V microplate reader. ROS production data are reported as a percent increase relative to negative controls (100%) with background fluorescence of cells not treated with HDCF-DA subtracted.

To verify that the iron nanoparticles did not react with HDCF-DA and to demonstrate oxidation of HDCF, additional control experiments were performed in cell-free solutions with

HDCF-DA and HDCF exposed to nZVI, Fe(II) and weathered nZVI. HDCF was prepared from HDCF-DA as described previously [24]. The appropriate iron concentration was added to 50 μM HDCF-DA or HDCF suspended in 20 mM phosphate (pH 7) in 1.5 mL microcentrifuge tubes. After 60 min in the dark, the suspensions were centrifuged and fluorescence was measured using a Turner Designs fluorometer (TD-700; $\lambda_{excitation}$ = 486 nm and $\lambda_{emission}$ = 510-700 nm).

Table S1. List of iron chelators and oxidant scavengers used in bronchial epithelial exposure experiments.

Compound	**Abbreviation**	**Function**
2,2'-bipyridine	BPY	Fe(II) chelator
Desferrioxamine B	DFO	Fe(II) and Fe(III) chelator
Dimethyl sulfoxide	DMSO	$OH^{\bullet}$ and Fe(IV) scavenger
Tert-butanol	TBA	$OH^{\bullet}$ scavenger
Benzoate	BA	$OH^{\bullet}$ scavenger

Discussion

Effect of phosphate, chloride, and bicarbonate on oxidant yield

Previous studies on nZVI indicate that the release and subsequent oxidation of Fe(II) by O_2 is the dominant mechanism of oxidant production at neutral pH values [1]. Ligands that accelerate the rate of Fe(II) oxidation or increase iron solubility were found to enhance oxidant production, with yields approaching theoretical maxima in some cases [2]. Because the bronchial epithelial cells can not tolerate PIPES, phosphate and bicarbonate buffers are often used in bioassays. Solution conditions used for exposures can affect oxidant production in reaction 5 through changes in iron coordination. In our system, oxidant production was approximately 2-3 times higher in PBS than PIPES, saline-PIPES, or HBSS (Figure S2). These findings can be explained by considering the effect of the ligands on Fe(II) oxidation rates and on iron solubility.

The enhancement in oxidant production observed in the presence of phosphate (Figure S5) may be attributable to the increase in filterable iron concentration with increasing phosphate concentrations (Figure S5). However, equilibrium calculations indicate that a solution of 100 μM Fe(II) or Fe(III) and 4 mM phosphate is oversaturated with $Fe_3(PO_4)_{2(s)}$ or ferrihydrite at pH 7 (Figure S7). In these experiments filterable iron decreased by 20% between 60 min and 6 h in PBS (data not shown), suggesting that iron precipitation occurs slowly in the presence of 4 mM phosphate.

The impact of chloride on oxidant yield was also investigated. The $FeCl^+$ species is less reactive than $FeOH^+$ and $Fe(OH)_2^0$ with O_2, resulting in a decrease in the rate of Fe(II) oxidation by O_2 of approximately 85% at pH 7 in the presence of 155 mM chloride in homogeneous solutions [25-26]. In our experiments, oxidant yield at 60 min decreased with increasing $[Cl^-]$ when PIPES was used as a buffer (Figure S4). Fe(II) oxidation in the presence of 155 mM Cl^-

was complete within 120 min, and observed HCHO production after 120 min was similar to values measured in PIPES alone at 60 min (data not shown). When phosphate was used as a buffer, the addition of chloride had a minimal effect on HCHO production (Figure S4) because Fe(II)-phosphate complexes dominated Fe(II) speciation (Figure S7).

To compare results from this study with previous research in which bicarbonate-containing solutions, such as HBSS [27-28], were used, the effect of HCO_3^- on iron speciation and reactivity was evaluated. While bicarbonate can significantly accelerate Fe(II) oxidation due to the formation of highly reactive species, such as $Fe(CO_3)_2^{2-}$ [26], elevated concentrations of HCO_3^- also can lead to formation of $FeCO_{3(s)}$. Under the experimental conditions employed in our study, HCHO production decreased when bicarbonate was added to PBS (Figure S3) due to slightly decreased iron solubility at $[HCO_3^-]$ >1 mM (data not shown). Although it is difficult to directly compare these results to conditions in lungs because epithelial lining fluid contains iron transport proteins [29] and antioxidants, such as ascorbic acid and glutathione [30], PBS is more likely to be more representative of conditions encountered *in vivo* than HBSS with respect to bicarbonate. The bicarbonate concentration in HBSS (i.e., >4 mM) is higher than the concentration encountered in air-saturated solutions and lowers oxidant production through Fe(II) precipitation.

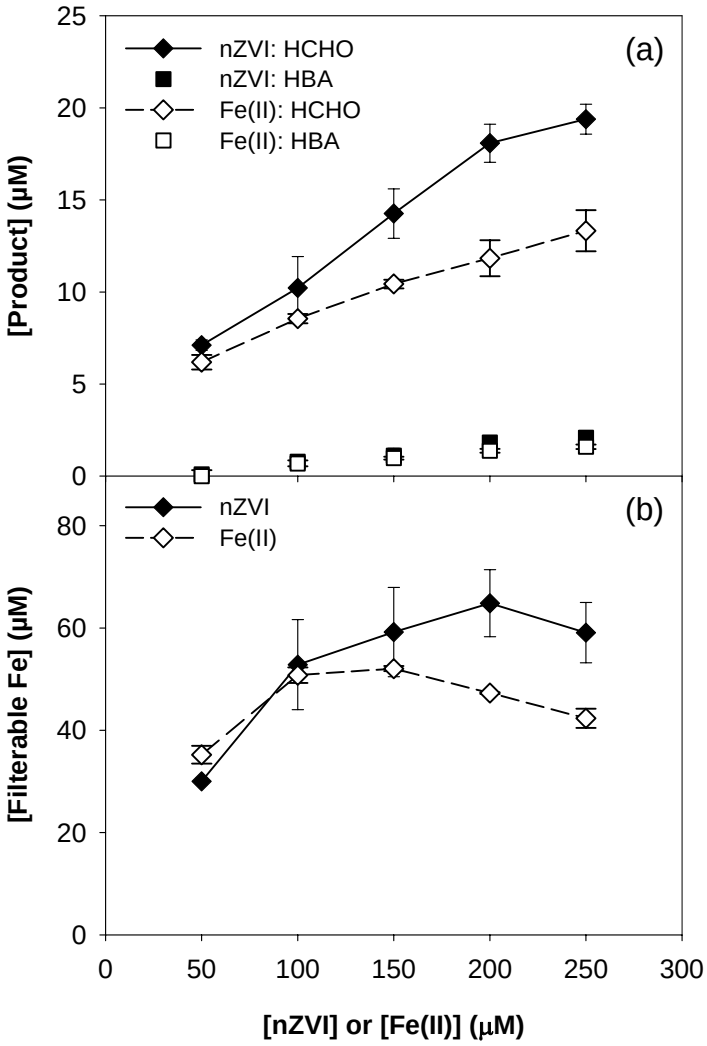

Figure S1. (a) HCHO or HBA production by nZVI or Fe(II) in PBS and 100 mM CH_3OH or 5 mM benzoate at pH 7, t = 60 min. (b) Filterable Fe present after 60 min of nZVI or Fe(II) oxidation in PBS and 100 mM CH_3OH at pH 7, t = 60 min. Note that no filterable Fe(II) was measured at 60 min under these conditions.

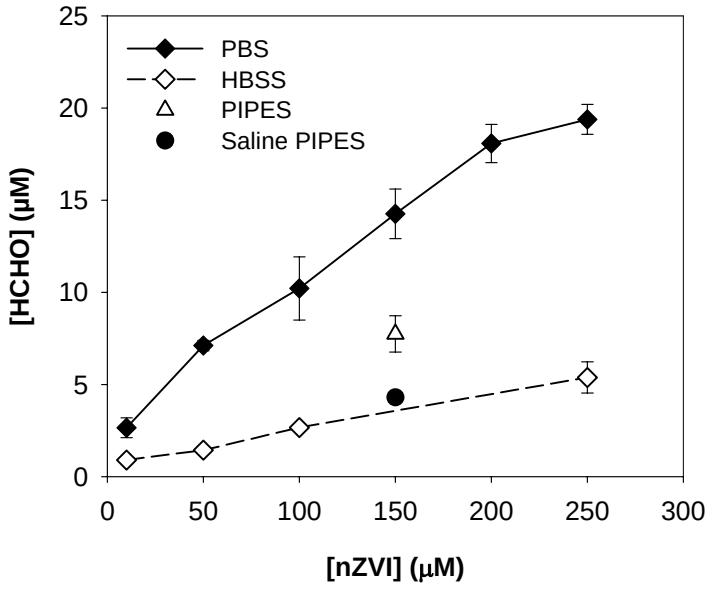

Figure S2. HCHO production by nZVI in 100 mM CH_3OH and PBS, HBSS, 1 mM PIPES, or 1 mM PIPES + 150 mM NaCl at pH 7, t = 60 min.

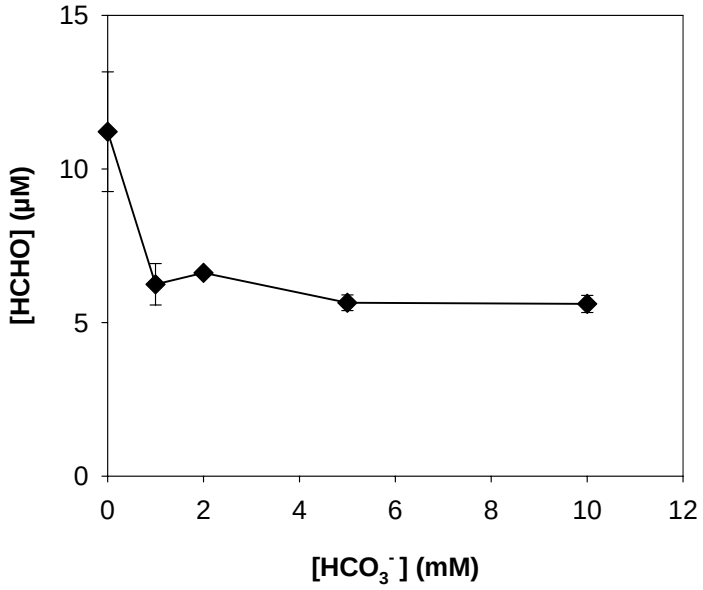

Figure S3. HCHO production by 100 μM nZVI in PBS and 100 mM CH_3OH with 0-10 mM HCO_3^- at pH 7, t = 60 min.

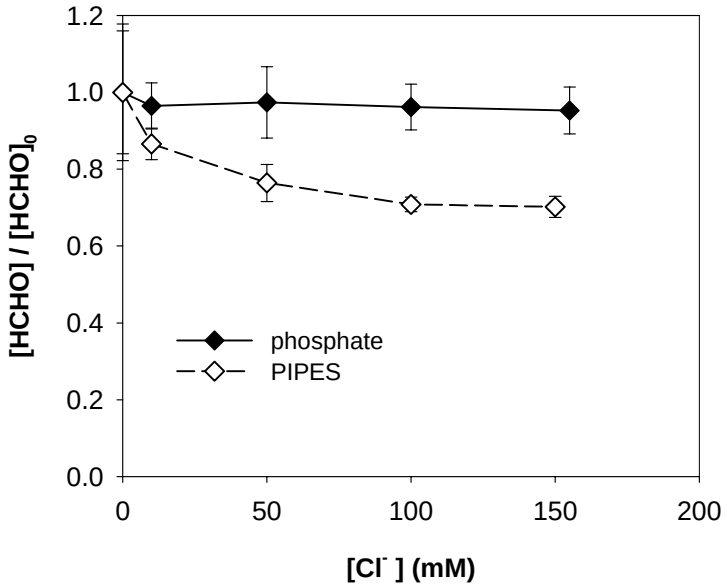

Figure S4. HCHO production by 100 μM nZVI in 4 mM phosphate or 2 mM PIPES and 100 mM CH_3OH with 0-155 mM Cl^- at pH 7, t = 60 min. $[HCHO]_0$ was 10.2 and 4.1 μM in phosphate and PIPES, respectively.

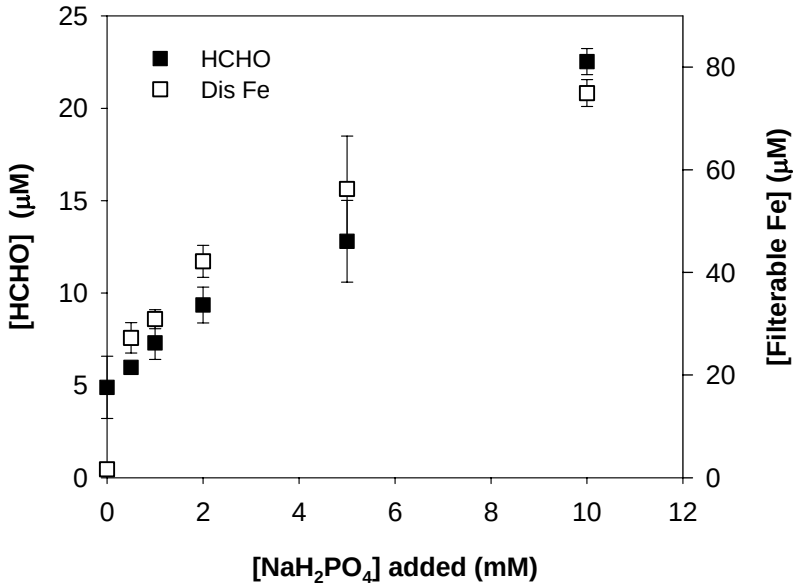

Figure S5. HCHO production and filterable Fe released by 150 μM nZVI in 1 mM PIPES and 100 mM CH_3OH with 0-10 mM NaH_2PO_4 at pH 7, t = 60 min.

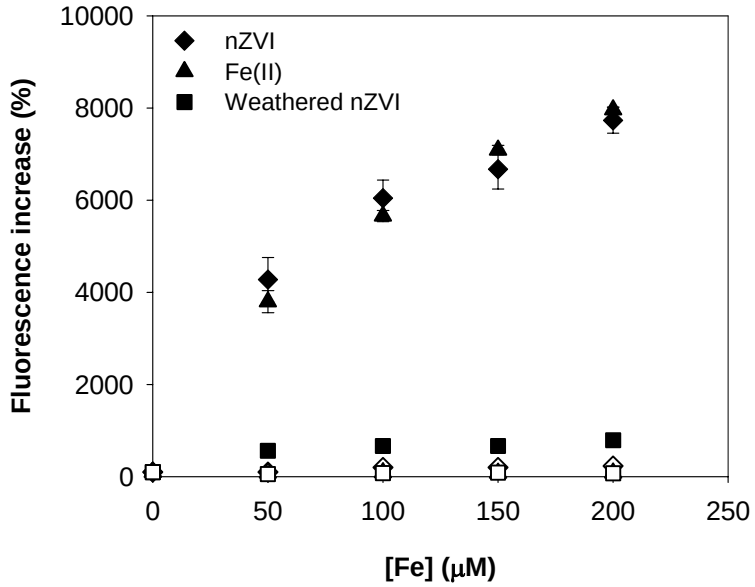

Figure S6. Reaction of nZVI, Fe(II), or weathered nZVI with 50 μM HDCF (solid points) or HDCF-DA (hollow points) in 20 mM phosphate at pH 7, t = 60 min. Data is reported as % increase relative to blank controls.

Table S2. Ratio of lung cell viability in cells exposed to 100-200 μM nZVI in 1 mM DMSO in PBS, 1 mM tert-butanol (TBA) in PBS, or 1 mM benzoate (BA) in PBS relative to viability in scavenger-free PBS. Experiments were conducted in PBS at pH 7, t = 60 min. DMSO data were collected in two batches of cells.

[nZVI] (μM)	DMSO	TBA	BA
100 μM	1.23 ± 0.08	1.00 ± 0.04	0.99 ± 0.06
200 μM	26.8 ± 22.3	0.97 ± 0.05	1.01 ± 0.06

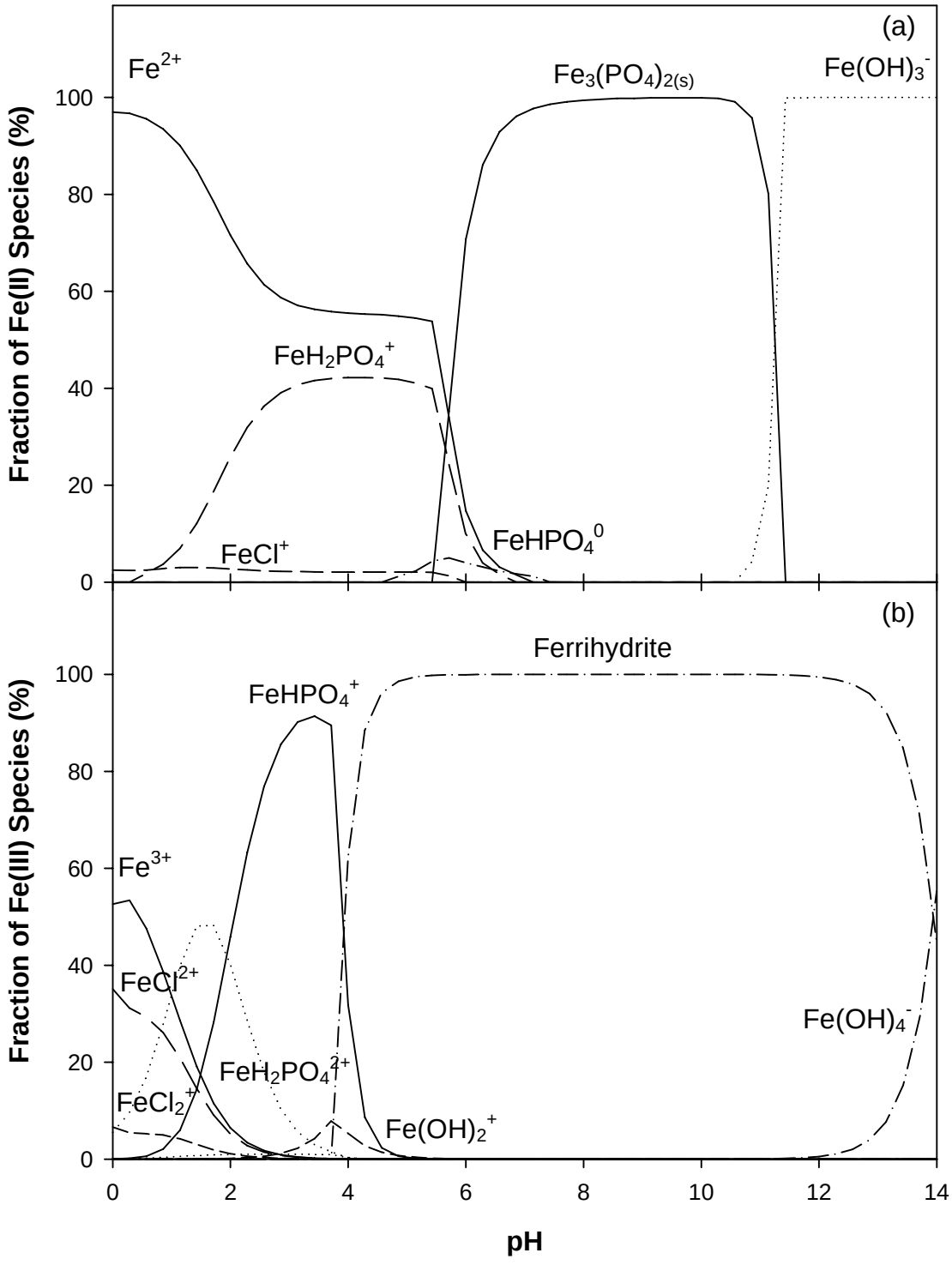

Figure S7. (a) Fe(II) and (b) Fe(III) equilibrium speciation in PBS.

References

1. Keenan, C. R.; Sedlak, D. L., Factors affecting the yield of oxidants from the reaction of nanoparticulate zero-valent iron and oxygen. *Environ. Sci. Technol.* **2008**, *42*, 1262-1267.

2. Keenan, C. R.; Sedlak, D. L., Ligand-enhanced reactive oxidant generation by nanoparticulate zero-valent iron and oxygen. *Environ. Sci. Technol.* **2008**, *42*, 6936-6941.

3. Nurmi, J. T.; Tratnyek, P. G.; Sarathy, V.; Baer, D. R.; Amonette, J. E.; Pecher, K.; Wang, C. M.; Linehan, J. C.; Matson, D. W.; Penn, R. L.; Driessen, M. D., Characterization and properties of metallic iron nanoparticles: Spectroscopy, electrochemistry, and kinetics. *Environ. Sci. Technol.* **2005**, *39*, 1221-1230.

4. Wang, C. B.; Zhang, W., Synthesizing nanoscale iron particles for rapid and complete dechlorination of TCE and PCBs. *Environ. Sci. Technol.* **1997**, *31*, 2154-2156.

5. Smith, R. M.; Martell, A. E., Eds. NIST Critically Selected Stability Constants of Metal Complexes Database, Version 8.0. National Institute of Standards and Technology, Gaithersburg, MD: 2004.

6. Voelker, B. M.; Sulzberger, B., Effects of fulvic acid on Fe (II) oxidation by hydrogen peroxide. *Environ. Sci. Technol.* **1996**, *30*, 1106-1114.

7. Nguyen, T. H.; Shannon, P. J.; Hoggard, P. E., Kinetics of the photooxidation of tris(bipyridine)iron(II) in chloroform. *Inorg. Chim. Acta* **1999**, *291*, 136-141.

8. Monzyk, B.; Crumbliss, A., Kinetics and mechanism of the stepwise dissociation of iron(III) from ferrioxamine B in aqueous acid. *J. Am. Chem. Soc.* **1982**, *104*, 4921-4929.

9. Hotze, E. M.; Labille, J.; Alvarez, P.; Wiesner, M. R., Mechanisms of photochemistry and reactive oxygen production by fullerene suspensions in water. *Environ. Sci. Technol.* **2008**, *42*, 4175-4180.

10. Sutherland, M. W.; Learmonth, B. A., The tetrazolium dyes MTS and XTT provide new quantitative assays for superoxide and superoxide dismutase. *Free Radical Res.* **1997**, *27*, 283-289.

11. Katsoyiannis, I. A.; Ruettimann, T.; Hug, S. J., pH dependence of Fenton reagent generation and As(III) oxidation and removal by corrosion of zero valent iron in aerated water. *Environ. Sci. Technol.* **2008**, *42*, 7424-7430.

12. Bader, H.; Sturzenegger, V.; Hoigne, J., Photometric method for the determination of low concentrations of hydrogen peroxide by the peroxidase catalyzed oxidation of N,N-diethyl-p-phenylenediamine (DPD). *Water Res.* **1988**, *22*, 1109-1115.

13. Zhou, X.; Mopper, K., Determination of photochemically produced hydroxyl radicals in seawater and freshwater. *Mar. Chem.* **1990**, *30*, 71-88.

14. Boland, S.; Baeza-Squiban, A.; Fournier, T.; Houcine, O.; Gendron, M.; Chervrier, M.; Jouvenot, G.; Coste, A.; Aubrier, M.; Marano, F., Diesel exhaust particles are taken up by human airway epithelial cells in vitro and alter cytokine production. *Am. J. Physiol. Lung Cell Mol. Physiol.* **1999,** *276*, 604-613.

15. Holder, A. L.; Lucas, D.; Goth-Goldstein, R.; Koshland, C. P., Inflammatory response of lung cells exposed to whole, filtered, and hydrocarbon denuded diesel exhaust. *Chemosphere* **2007**, *70,* 13-19.

16. Holder, A. L.; Lucas, D.; Goth-Goldstein, R.; Koshland, C. P., Cellular response to diesel exhaust particles strongly depends on the exposure method. *Toxicol. Sci.* **2008,** *103*, 108-115.

17. Canal-Raffin, M.; l'Azou, B.; Jorly, J.; Hurtier, A.; Cambar, J.; Brochard, P., Cytotoxicity of folpet fungicide on human bronchial epithelial cells. *Toxicology* **2008,** *249*, 160-166.

18. van der Deen, M.; Homan, S.; Timmer-Bosscha, H.; Scheper, R. J.; Timens, W.; Postma, D. S.; de Vries, E. G., Effect of COPD treatments on MRP1-mediated transport in bronchial epithelial cells. *Int. J. Chron. Obstruct. Pulmon. Dis.* **2008,** *3*, 469-475.

19. Jeulin, C.; Dazy, A. C.; Marano, F., Effects of hydrogen peroxide and hydroxyl radicals on the cytosolic side of anion-selective cation channel in the cultured human bronchial epithelial cell line 16HBE14o-. *Pflugers Arch.* **2002,** *443*, 574-583.

20. Halliwell, B.; Whiteman, M., Measuring reactive species and oxidative damage in vivo and in cell culture: How should you do it and what do the results mean? *Brit. J. Pharmacol.* **2004**, *142*, 231-255.

21. Jakubowski, W.; Bartosz, G., 2,7-Dichlorofluorescin oxidation and reactive oxygen species: What does it measure? *Cell Bio. Int.* **2000**, *24*, 757-760.

22. Keller, A.; Mohamed, A.; Dröse, S.; Brandt, U.; Fleming, I.; Brandes, R., Analysis of dichlorodihydrofluorescein and dihydrocalcein as probes for the detection of intracellular reactive oxygen species. *Free Radical Res.* **2004**, *38*, 1257-1267.

23. Limbach, L. K.; Wick, P.; Manser, P.; Grass, R. N.; Bruinink, A.; Stark, W. J., Exposure of engineered nanoparticles to human lung epithelial cells: Influence of chemical composition and catalytic activity on oxidative stress. *Environ. Sci. Technol.* **2007**, *41*, 4158-4163.

24. Cathcart, R.; Schwiers, E.; Ames, B. N., Detection of picomole levels of hydroperoxides using a fluorescent dichlorofluorescein assay. *Anal. Biochem.* **1983**, *134*, 111-116.

25. Millero, F. J.; Izaguirre, M., Effect of ionic strength and ionic interactions on the oxidaiton of Fe(II). *J. Sol. Chem.* **1989,** *18*, 585-599.

26. King, D. W., Role of carbonate speciation on the oxidation rate of Fe (II) in aquatic systems. *Environ. Sci. Technol.* **1998,** *32*, 2997-3003.

27. Phenrat, T.; Long, T. C.; Lowry, G. V.; Veronesi, B., Partial oxidation ("aging") and surface modification decrease the toxicity of nanosized zerovalent iron. *Environ. Sci. Technol.* **2009,** *43*, 195-200.

28. Limbach, L.; Wick, P.; Manser, P.; Grass, R.; Bruinink, A.; Stark, W., Exposure of Engineered Nanoparticles to Human Lung Epithelial Cells: Influence of Chemical Composition and Catalytic Activity on Oxidative Stress Supporting Information. *Environ. Sci. Technol.* **2007,** *41*, 4158-63.

29. Turi, J. L.; Yang, F.; Garrick, M. D.; Piantadosi, C. A., The iron cycle and oxidative stress in the lung. *Free Radical Bio. Med.* **2004,** *36*, 850-857.

30. Sun, G.; Crissman, K.; Norwood, J.; Richards, J.; Slade, R.; Hatch, G. E., Oxidative interactions of synthetic lung epithelial lining fluid with metal-containing particulate matter. *Am. J. Physiol. Lung Cell. Mol. Physiol.* **2001,** *281*, 807-815.